ISSN 0036-0236, Russian Journal of Inorganic Chemistry, 2026, Vol. 71, No. 5, pp. 650–656. © Pleiades Publishing, Ltd., 2026.

PHYSICOCHEMISTRY OF SOLUTIONS

Effect of Magnesium Cations on the Thermal Stability of Solid Solutions of Molecular Hydrogen in Silicates

V. S. Efimchenko[a], *, K. P. Meletov[a], M. A. Korotkova[a], and N. S. Sukhinina[a]

[a] *Osipyan Institute of Solid State Physics, Russian Academy of Sciences, Chernogolovka, Moscow oblast, 142432 Russia*

**e-mail: efimchen@issp.ac.ru*

Received February 2, 2026; revised March 12, 2026; accepted March 13, 2026

Abstract—The effect of magnesium cations on the thermal stability of $Mg_{0.6}SiO_{2.6}$–$0.34H_2$ and $Mg_{0.5}SiO_{2.5}$–$0.35H_2$ molecular hydrogen solid solutions was studied. The hydrogen-loss kinetics was determined from the evolution of Raman spectra. The temperature dependence $1/T$ of decay time constant τ is well described by the Arrhenius equation with activation energies of 59.5 ± 2.9 and 19.2 ± 1.4 kJ/mol at magnesium contents of 0.6 and 0.5, respectively. The large difference between the activation energies indicates a strong influence of the H_2/Mg^{2+} ratio on the electrostatic interaction of hydrogen molecules with magnesium cations. The highest value of activation energy $E_A = 59.5 \pm 2.9$ kJ/mol obtained for the ratio $H_2/Mg^{2+} = 0.56$ made it possible to increase the desorption temperature of H_2 to 293–340 K, which is necessary for using the material for solid-state hydrogen storage.

Keywords: desorption, hydrogen storage, activation energy

DOI: 10.1134/S0036023626600802

INTRODUCTION

Magnesium is a promising material for use as a container for hydrogen, since the MgH_2 compound contains 7.65 wt % H_2. However, due to the high desorption temperature of 573 K [1] and the deterioration of the adsorption kinetics upon repeated hydrogenation, the MgH_2 compound has found no practical application to date. To reduce the temperature and increase the rate of hydrogen adsorption/desorption from MgH_2, in a number of studies, the material was ground in ball mills and/or alloyed with various elements and compounds that reduce the binding energy between hydrogen and matrix atoms [2–6]. However, none of these methods led to a decrease in the dehydrogenation temperature of MgH_2 up to the optimal interval of 263–373 K, since the hydrogen was still bound to magnesium by a strong ionic–covalent bond. The closest desorption temperature to this range (373 K) was achieved in a composite of magnesium hydride with single-wall carbon nanotubes [7].

Our previous experiments showed that the decomposition of a solid solution of hydrogen in lithium silicate glass at atmospheric pressure occurs in the temperature range of 273–363 K [8]. Despite the high value of activation energy of solution decomposition $E_A = 40.4 \pm 1.8$ kJ/mol, obtained from the temperature dependence of the Raman spectra, hydrogen retains its molecular form and does not form new chemical bonds with the silicate lattice. It is assumed that the high thermal stability of a molecular solution of hydrogen in lithium–silicate glass is due to the occurrence of a Kubas interaction [9] between lithium cations and hydrogen molecules or to an interaction similar in nature to, but greater in magnitude than the van der Waals interaction. According to theoretical calculations, similar interactions can also occur with cations of other alkaline, alkaline earth and transition elements [10–15]. Since the radius of Mg^{2+} cations ($r = 0.72$ Å) is close to the radius of lithium cations ($r = 0.76$ Å), one can assume that they may be close to their interaction energies with hydrogen molecules. We have previously shown that, in Mg_ySiO_{2+y} amorphous magnesium silicates ($y = 0.5$–0.89), a fairly large amount of hydrogen is dissolved in molecular form [16]. According to thermal desorption data of $Mg_ySiO_{2+y}\cdot XH_2$, more than 50% of hydrogen is released at temperatures >273 K, which may indirectly indicate a stronger interaction between H_2 and magnesium cations compared to van der Waals interaction.

The aim of this work is to study the thermal stability of molecular hydrogen solutions with different magnesium cation contents at normal pressure. For this purpose, the kinetics of decomposition of solid solutions of $Mg_{0.6}SiO_{2.6}$–$0.34H_2$ and $Mg_{0.5}SiO_{2.5}$–$0.35H_2$ was studied, the activation energy was determined, and the characteristic times of their decay at different temperatures were identified using Raman spectroscopy.

EXPERIMENTAL

The initial samples of amorphous magnesium silicates were synthesized by the sol–gel method according to [17]. The original samples were studied by powder X-ray diffraction at normal pressure and room temperature on a Siemens D500 diffractometer (Siemens, Germany) using CuK_α-radiation isolated using a monochromator. The obtained X-ray diffraction spectra corresponded to the amorphous structure of the original magnesium silicate samples and did not contain crystalline lines. Elemental analysis of the samples carried out by X-ray microanalysis on a Supra 50VP scanning electron microscope with an EDS-Oxford Inca Energy 450 microanalysis system (Carl Zeiss, Germany) determined their composition as $Mg_{0.5}SiO_{2.5}$ and $Mg_{0.6}SiO_{2.6}$. Saturation of the initial samples of amorphous magnesium silicates with hydrogen was carried out in toroid-type chambers at a pressure of 7.5 GPa and a temperature of 523 K, followed by quenching to liquid-nitrogen temperature and a reduction in pressure to atmospheric pressure. The samples obtained in this way were stored in liquid nitrogen until further use [18, 19].

The amount of dissolved hydrogen was determined by thermal desorption in a pre-evacuated chamber with a calibrated volume. According to the data obtained, $Mg_{0.5}SiO_{2.5}$ and $Mg_{0.6}SiO_{2.6}$ contained 0.35 and 0.34 mol of hydrogen, respectively, after hydrogenation, which is consistent with previously obtained data on the solubility and release of hydrogen in these compounds [16].

The patterns of hydrogen desorption at different temperatures were studied in situ on the change in the Raman spectra of hydrogen-saturated amorphous magnesium silicates in the isothermal annealing mode at atmospheric pressure. Raman spectra were recorded at a temperature of 80 K using a nitrogen cryostat of our own design with loading of samples without intermediate heating [20]. The cryostat was equipped with a temperature controller and a resistive heater, providing temperature stabilization in the range from 80 to 390 K with an accuracy of ±0.4 K. Spectra were recorded in backscattering geometry using a setup consisting of a SpectraPro-2500i spectrograph (Acton Research Corp., United States) and a Pixis2K CCD matrix (Princeton Instruments, United States). The 532-nm line of a continuous single-mode diode-pumped laser was focused onto the sample with an Olympus BX51 microscope (OLYMPUS Co., Japan) using a 50× objective. The spatial resolution was ~1.5 μm, and the spectral resolution was 3.2/4.1 cm^{-1} in the spectral region of 685/532 nm. The laser line in the scattered radiation was suppressed by an edge filter with OD = 6 and a passband of ~60 cm^{-1}, with the beam intensity in front of the sample being ~5 mW.

RESULTS AND DISCUSSION

Raman Spectra of $Mg_{0.6}SiO_{2.6}$–$0.34H_2$ and $Mg_{0.5}SiO_{2.5}$–$0.35H_2$ Hydrogen Solutions

Figure 1 shows the Raman spectrum of the $Mg_{0.6}SiO_{2.6}$–$0.34H_2$ sample in the frequency range of 200–4250 cm^{-1} obtained at liquid-nitrogen temperature and atmospheric pressure. The narrow peak at 4163 cm^{-1} in the spectrum of the sample corresponds to H–H-vibrational modes $Q1(0)$ of hydrogen molecules dissolved in amorphous $Mg_{0.6}SiO_{2.6}$. The lines at 328.5 and 590 cm^{-1} correspond to rotational modes $S(0)$ of hydrogen. In addition to the molecular hydrogen lines, the spectrum also contains characteristic magnesium silicate lines at 800–1200 cm^{-1} and lines of vibrational O–H oscillations of water and hydroxyl groups at 3200–3600 cm^{-1}, the presence of which is due to the deposition of water ice on the surface of the sample at a temperature of 80 K. A similar spectrum with lines of molecular hydrogen is also observed for a solution of $Mg_{0.5}SiO_{2.5}$–$0.35H_2$.

A weak intensity of silicate lines in the Raman spectrum in the region <800 cm^{-1}, which is associated with noticeable depolymerization of the silicate lattice, for Mg_ySiO_{2+y} amorphous magnesium silicates with $y > 0.33$ [16]. Therefore, determination of the relative change in the intensity of rotational hydrogen lines, which was previously used to study the kinetics of decomposition of solid hydrogen solutions, is difficult due to the weakness of the silicate lines and the impossibility of using them as a reference [21]. Another method for determining characteristic decay times is to measure the time dependences of the intensity or frequency of the vibrational line of molecular hydrogen, which we proposed in [8, 22]. Note that both the intensity and frequency of the vibrational line of hydrogen in the $Mg_{0.6}SiO_{2.6}$–$0.34H_2$ solution remained virtually unchanged during the experiment (~1 h) at temperatures from 80 to 293 K, indicating a relatively high stability of the samples under these conditions. At the same time, as can be seen from Fig. 1, when the sample is heated to 297 K, the width of the vibrational H–H mode increases significantly due to the contribution increasing with temperature of *ortho*-hydrogen in its intensity (Fig. 1).

Kinetics of decomposition of $Mg_{0.6}SiO_{2.6}$–$0.34H_2$ and $Mg_{0.5}SiO_{2.5}$–$0.35H_2$ Solutions

The kinetics of hydrogen desorption during isothermal annealing of amorphous magnesium silicates was determined not by the position of the vibrational band of the H_2 molecule, but by the change in its overall intensity depending on the annealing time. Figure 2 shows the Raman spectra of the vibrational band and the dependence of its intensity on the annealing time at a temperature of 328 K (insert). An exponential decrease in the amount of dissolved hydrogen is

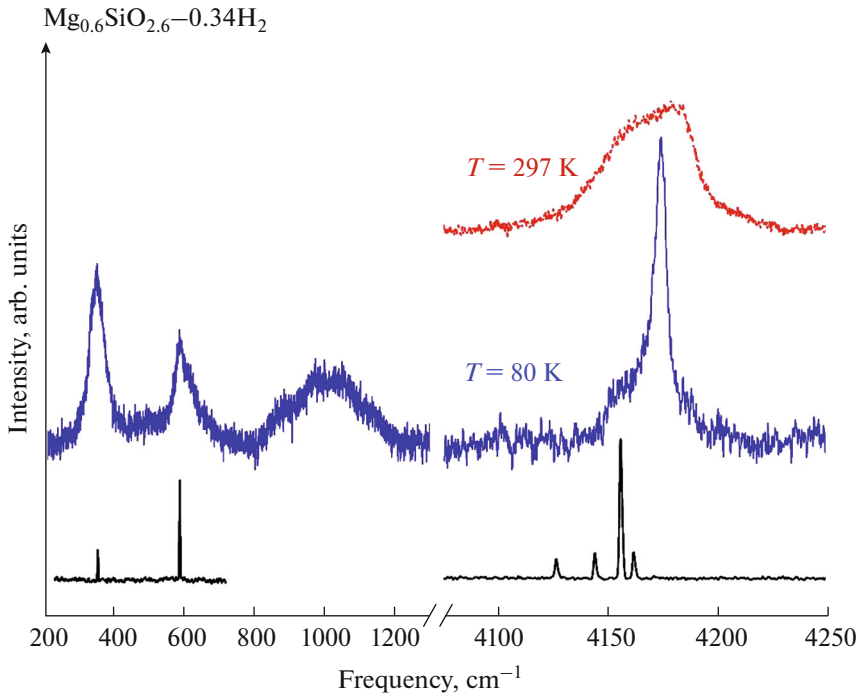

Fig. 1. Raman spectra of the solid solution of hydrogen $Mg_{0.6}SiO_{2.6}$–0.34H_2 at normal pressure and 297 (top) and 80 K (middle) and gaseous hydrogen at 30 atm and room temperature (bottom).

observed with annealing time, with the dependence reaching a plateau 0.5 h after the start of annealing. The plateau is associated with the peculiarities of Raman spectra measurements in backscattering geometry, when the signal is recorded from the near-surface region of the samples. Saturation is due to the fact that the diffusion of hydrogen from the depth of the sample after some time compensates for its desorption from the near-surface region [21].

The background signal associated with the emission of defects formed during the synthesis of samples was presubtracted from the experimental spectra. The intensity of the vibrational H–H band of the spectrum was always normalized to the background luminescence signal at a frequency of 4000 cm^{-1}, which made it possible to minimize the error due to possible deviation from the initial focusing in the excitation spot.

The inset to Fig. 3 shows the characteristic intensity dependences of the H–H vibration line from the annealing time for samples $Mg_{0.6}SiO_{2.6}$–0.34H_2 obtained at different temperatures in the range of 293–340 K. All data on hydrogen desorption in $Mg_{0.6}SiO_{2.6}$–0.34H_2 obtained at different temperatures are well approximated by an exponential function $I_{H_2} = A \times \exp(-t/\tau) + B$ with time constant τ and coefficients A and B varying from $\tau = 9770 \pm 2500$ s, $B = 0.52 \pm 0.1$, $A = 0.48 \pm 0.1$ at $T = 293$ K to $\tau = 240 \pm 66$ s, $B = 0.25 \pm 0.08$, $A = 0.75 \pm 0.06$ at $T = 340$ K. The obtained dependences indicate the activation nature of hydrogen desorption in the $Mg_{0.6}SiO_{2.6}$–0.34H_2 sample. The same dependences were obtained for the $Mg_{0.5}SiO_{2.5}$–0.35H_2 solution in the temperature range of 168–222 K. Figure 3 also shows the dependence of the values of τ on the reciprocal temperature $1/K_BT$ and their approximation by Arrhenius dependence $\tau(T) = A \times \exp(E_A/K_BT)$ for $Mg_{0.6}SiO_{2.6}$–0.34H_2 (circles) and $Mg_{0.5}SiO_{2.5}$–0.35H_2 (hexagons) solutions.

The activation energy of decomposition of a solid hydrogen solution $Mg_{0.6}SiO_{2.6}$–0.34H_2 ($E_a = 59.5 \pm 2.9$ kJ/mol) is significantly greater than the activation energy for the decomposition of hydrogen solution in lithium silicate glass ($E_a = 40.4 \pm 1.8$ kJ/mol) [8]. The value of activation energy $E_a = 59.5 \pm 2.9$ kJ/mol is the maximum for all known solid solutions of molecular hydrogen, which is the reason for the high thermal stability of the $Mg_{0.6}SiO_{2.6}$–0.34H_2 solution under normal conditions.

Despite the close magnesium content and almost the same amount of dissolved hydrogen, the activation energy of decomposition of the $Mg_{0.5}SiO_{2.5}$–0.35H_2 solution has a magnitude several times smaller $E_a = 19.2 \pm 1.4$ kJ/mol, which is close to activation energy of hydrogen desorption from silica glass $E_A = 15.44 \pm 0.96$ kJ/mol [21]. For this reason, under normal conditions, the $Mg_{0.5}SiO_{2.5}$–0.35H_2 solution has a rather low thermal stability, losing almost all of its dissolved hydrogen within a few seconds.

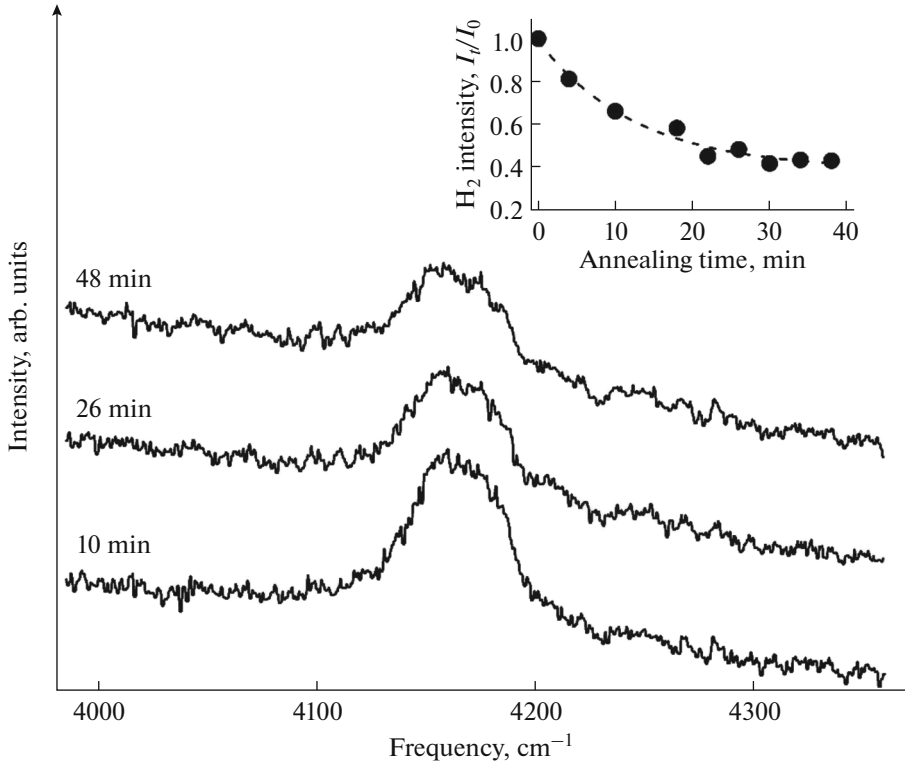

Fig. 2. Raman spectra of the solid solution of hydrogen $Mg_{0.6}SiO_{2.6}$–$0.34H_2$ in the region of the H–H vibration band of the H_2 molecule after 10, 26, and 48 min of annealing at T = 328 K. Inset: (dots) dependence of the band intensity on the annealing time; (dashed line) approximation with an exponential function.

Interaction of Hydrogen with Magnesium Cations in Amorphous Silicates

Since the activation energy of decomposition of the $Mg_{0.6}SiO_{2.6}$–$0.34H_2$ solution ($E_A = 59.5 \pm 2.9$ kJ/mol) is more than the van der Waals interaction energy (E = 4.8–9.65 kJ/mol), it can be assumed that the interaction of H_2 molecules with silicate atoms is stronger than van der Waals. Such an interaction can be of Kubas type, which has a characteristic energy value in the range 9.65–77.19 kJ/mol [23]. A typical example of the Kubas forces is the interaction between the H_2 molecule and transition metal atoms, resulting from the hybridization of the σ-orbital of the H_2 molecule and *d*-orbitals of the transition element atom [24, 25]. Kubas-type interactions lead to an elongation of the H–H bond in the hydrogen molecule by ~20% and a decrease in the frequency of the vibrational mode to 3400–3600 cm^{-1} [25]. It should be noted that, in the present work, no decrease in the frequency of the vibrational H–H mode was observed for H_2 molecules in amorphous magnesium silicate. On the contrary, the frequency of this mode (4163 cm^{-1}) is significantly higher than the frequency (4155 cm^{-1}) of the vibrational mode of free molecular hydrogen [21]. A significantly greater increase in the frequency of the vibrational mode H_2 (up to 4191 cm^{-1}) was observed for solutions of hydrogen in lithium–silicate glass [8]. These data indicate that the enhancement of the H_2 interaction with cations of alkali and alkaline earth elements can occur with the help of a different type of bond between the hydrogen molecule and the cations, which differs from a Kubas-type bond. Indeed, according to first-principles calculations [14], a lithium cation located on the surface of a BHNH layer can hold up to four hydrogen molecules. The binding energy of H_2 molecules with the atoms of the lithium-modified BHNH layer is close in magnitude to the energy characteristic of the Kubas interaction and is in the preferred range 9.65–77.19 kJ/mol. However, unlike systems with a Kubas-type interaction, in this case the hydrogen molecule acquires a negative charge due to the partial transfer of electron density to it from the lithium cation, which leads to an increase in its electrostatic interaction with the BNHN layer. A similar type of enhancement of electrostatic interaction with hydrogen molecules has been proposed for carbon materials such as enyne and silicographene doped with cations of other alkali and alkaline earth elements [26, 27]. These studies lack data on the possible change in the H–H bond length of the hydrogen molecule due to charge transfer and increased electrostatic

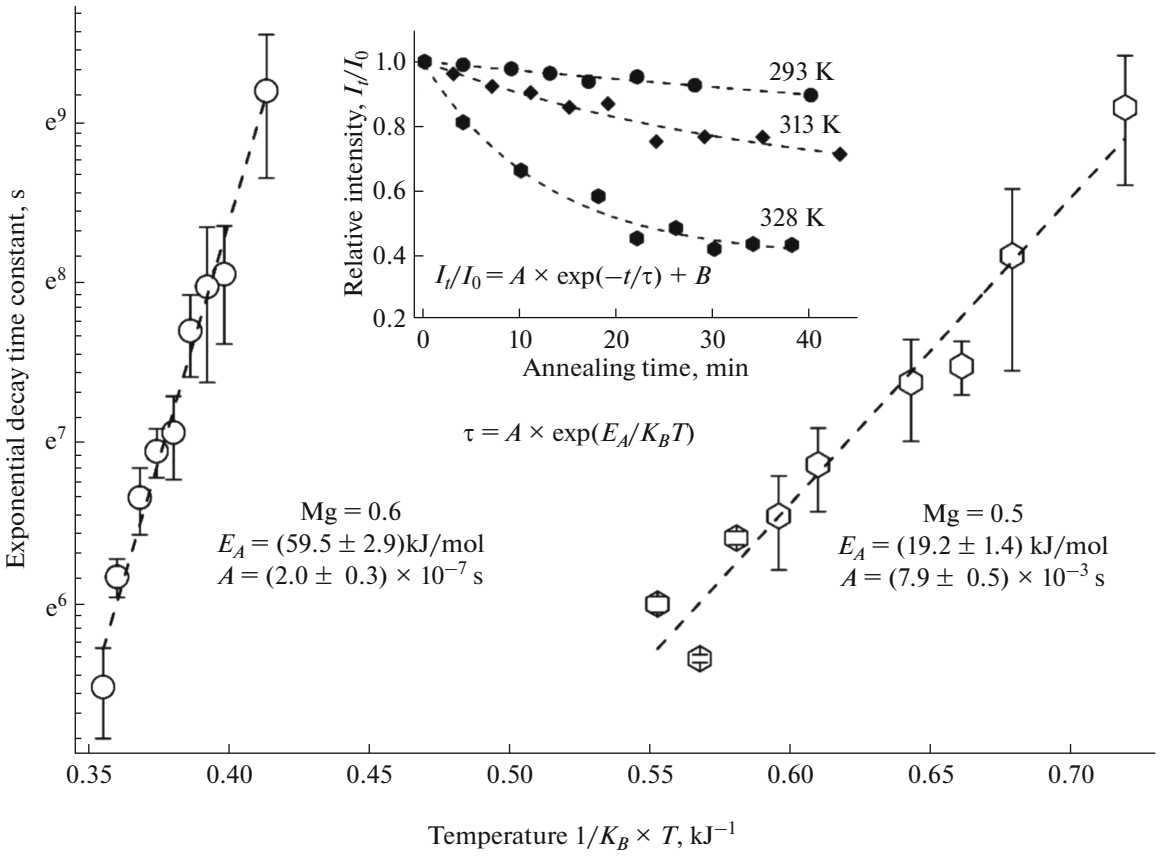

Fig. 3. Arrhenius dependence $\tau(T) = A \times \exp(E_A/K_BT)$ of exponential decay time constant τ on the annealing temperature $1/K_BT$ (symbols) and its linear approximation (dashed line). Right—$Mg_{0.5}SiO_{2.5}$–$0.35H_2$; left—$Mg_{0.6}SiO_{2.6}$–$0.34H_2$. Inset: dependence of the intensity of the H–H vibration mode on the annealing time in the $Mg_{0.6}SiO_{2.6}$–$0.34H_2$ sample at 293, 313, and 328 K (circles, diamonds, and hexagons, respectively). Dashed line: approximation by the exponential decay function.

interaction with surrounding atoms. If we assume that the H–H bond length can decrease when the H_2 molecule acquires additional electron density, then the frequency of its vibrational mode must increase. It is precisely this effect that is observed in the present work, as well as in previously studied solid solutions of hydrogen in lithium–silicate glass [8].

Despite the almost equal amount of dissolved hydrogen and close content of magnesium cations, the $Mg_{0.6}SiO_{2.6}$–$0.34H_2$ and $Mg_{0.5}SiO_{2.5}$–$0.35H_2$ solutions demonstrate different decay kinetics. One possible explanation for this may be different amounts of magnesium cations per hydrogen molecule. Previously, using the example of metal–organic lattices with magnesium cations, it was shown that, with an increase in the H_2/Mg^{2+} ratio from 0.8 to 1.1, there is a sudden drop in the isosteric heat of adsorption by more than two times—from $\Delta H = -10.7$ to ~–5 kJ/mol [28]. The reason for this is the decrease in the number of magnesium cations free to "bind" guest molecules with an increase in the hydrogen content. When a certain concentration of hydrogen is exceeded, only a portion of the H_2 molecules is associated with magnesium cations by high-energy interactions. It is possible that a similar effect occurs when hydrogen is dissolved in amorphous magnesium silicates. At the ratio $H_2/Mg^{2+} = 0.56$ in the $Mg_{0.6}SiO_{2.6}$–$0.34H_2$ solution, each hydrogen molecule is bound to an average of 1.76 magnesium cations by an interaction that has a higher binding energy than the van der Waals interaction.

When the ratio increases to $H_2/Mg^{2+} = 0.7$ in the $Mg_{0.5}SiO_{2.5}$–$0.35H_2$ solution, the number of magnesium cations associated with a hydrogen molecule drops to 1.43, which leads to a decrease in the average interaction energy between H_2 and silicate atoms. A significant portion of the hydrogen in such a solution may not form any bond with magnesium cations and has a bond energy with silicate close to the bond energy of hydrogen in silica glass.

CONCLUSIONS

The dependence of decay time constant τ on temperature $1/K_B \times T$ for the $Mg_{0.6}SiO_{2.6}$–$0.34H_2$ solu-

tion is well described by the Arrhenius equation with activation energy $E_A = 59.5 \pm 2.9$ kJ/mol. This is the maximum known value of the activation barrier for the release of molecular hydrogen from a solvent matrix under normal conditions. The significantly higher activation energy for hydrogen release from $Mg_{0.6}SiO_{2.6}$ compared to $E_A = 15.44 \pm 0.96$ kJ/mol hydrogen release from silica glass SiO_2 is associated with the transfer of part of the electron density from the magnesium cation to the hydrogen molecule and, accordingly, with the emergence of electrostatic interaction between the H_2 molecule and magnesium cations. With a lower magnesium content in the $Mg_{0.5}SiO_{2.5}$–$0.35H_2$ solution, activation energy of decay $E_A = 19.2 \pm 1.4$ kJ/mol is close to the activation energy of the decomposition of a hydrogen solution in pure silica glass, which indicates the predominance of van der Waals interaction between magnesium cations and H_2 in this solution. Thus, the data obtained in this work show that magnesium cations at a ratio of $Mg^{2+}/H_2 = 1.76$ are able to effectively hold hydrogen molecules. The electrostatic interaction that arises between magnesium cations and hydrogen molecules at this ratio leads to an increase in the activation energy to $E_A = 59.5 \pm 2.9$ kJ/mol and, thus, allows the hydrogen desorption temperature to be brought closer to the range of 293–340 K, which is more convenient for using the material as a solid-state hydrogen container.

AUTHOR CONTRIBUTION

All authors made a significant contribution to the development of the concept, conduct of the study, and preparation of the article.

FUNDING

The research was carried out within the framework of a state assignment of the Osipyan Institute of Solid State Physics, Russian Academy of Sciences.

CONFLICT OF INTEREST

The authors of this work declare that they have no conflicts of interest.

REFERENCES

1. P. B. Terent'ev, E. G. Gerasimov, N. V. Mushnikov, et al., Phys. Metals Metallogr. **116**, 1197 (2015). https://doi.org/10.1134/S0031918X15120121
2. J. Zhang, Z. Li, Y. Wu, et al., RSC Adv. **9**, 408 (2019). https://doi.org/10.1039/C8RA05596C
3. Q. Luo, J. Li, B. Li, et al., J. Magnes. Alloys **7**, 58 (2019). https://doi.org/10.1016/j.jma.2018.12.001
4. A. P. Baraban, A. P. Voyt, I. E. Gabis, et al., Crystallogr. Rep. **69**, 93 (2024). https://doi.org/10.1134/S1063774523601259
5. Y. Wu, Z. Yuan, Y. Zhang, et al., Inorg. Chem. **64**, 7607 (2025). https://doi.org/10.1021/acs.inorgchem.5c00604
6. A. S. Zyubin, T. S. Zyubina, O. V. Kravchenko, et al., Russ. J. Inorg. Chem. **70**, 1047 (2025). https://doi.org/10.1134/S0036023625601898
7. V. N. Kudiiarov, R. R. Elman, N. E. Kurdyumov, et al., J. Surf. Investig. **17**, 1295 (2023). https://doi.org/10.1134/S1027451023060101
8. V. S. Efimchenko, M. A. Korotkova, K. P. Meletov, et al., J. Phys. Chem. C **127**, 13538 (2023). https://doi.org/10.1021/acs.jpcc.3c02644
9. G. J. Kubas, R. R. Ryan, B. I. Swanson, et al., J. Am. Chem. Soc. **106**, 451 (1984). https://doi.org/10.1021/ja00314a049
10. J. G. Vitillo, L. Regli, S. Chavan, et al., J. Am. Chem. Soc. **130**, 8386 (2008). https://doi.org/10.1021/ja8007159
11. W. Zhou and T. Yildirim, J. Phys. Chem. C **112**, 8132 (2008). https://doi.org/10.1021/jp803350y
12. J. Niu, B. K. Rao and P. Jena, Phys. Rev. Lett. **68**, 2277 (1992). https://doi.org/10.1103/PhysRevLett.68.2277
13. Y. Liu, B. Su, W. Dong, et al., J. Am. Chem. Soc. **141**, 8358 (2019). https://doi.org/10.1021/jacs.9b03213
14. S. Bhattacharya, A. Bhattacharya, and G. P. Das, J. Phys. Chem. C **116**, 3840 (2012). https://doi.org/10.1021/jp210355n
15. C. Chung, J. Ihm and H. Lee, J. Korean Phys. Soc. **66**, 1649 (2015). https://doi.org/10.3938/jkps.66.1649
16. V. S. Efimchenko, N. V. Barkovskii, V. K. Fedotov, et al., J. Alloys Compd. **770**, 229 (2019). https://doi.org/10.1016/j.jallcom.2018.08.111
17. A. G. Kalampounias, Bull. Mater. Sci. **34**, 299 (2011). https://doi.org/10.1007/s12034-011-0064-x
18. L. G. Khvostantsev, V. N. Slesarev, and V. V. Brazhkin, High Press. Res. **24**, 371 (2004). https://doi.org/10.1080/08957950412331298761
19. V. E. Antonov, B. M. Bulychev, V. K. Fedotov, et al., Int. J. Hydrogen Energy **42**, 22454 (2017). https://doi.org/10.1016/j.ijhydene.2017.03.121
20. K. P. Meletov, Instrum. Exp. Tech. **63**, 291 (2020). https://doi.org/10.1134/S0020441220020013
21. K. P. Meletov and V. S. Efimchenko, Chem. Phys. Lett. **793**, 139477 (2022). https://doi.org/10.1016/j.cplett.2022.139477
22. K. P. Meletov, V. S. Efimchenko, M. A. Korotkova, et al., Int. J. Hydrogen Energy **48**, 14337 (2023). https://doi.org/10.1016/j.ijhydene.2022.12.297

23. Q. Lai, M. Paskevicius, D. A. Sheppard, et al., ChemSusChem **8**, 2789 (2015). https://doi.org/10.1002/cssc.201500231

24. C. V. J. Skipper, A. Hamaed, D. Antonelli, et al., Dalton Trans. **41**, 8515 (2012). https://doi.org/10.1039/c2dt30383c

25. K. I. M. Rojas, R. C. Villagracia, S. Narido, et al., Mater. Res. Express **6**, 055509 (2019). https://doi.org/10.1088/2053-1591/ab0294

26. E. Anikina, T. Hussain, V. Beskachko, et al., J. Phys. Chem. C **124**, 16827 (2020). https://doi.org/10.1021/acs.jpcc.0c04254

27. E. Anikina, T. Hussain, V. Beskachko, et al., Sustainable Energy Fuels **4**, 5578 (2020). https://doi.org/10.1039/d0se00852d

28. D. Gygi, E. D. Bloch, J. A. Mason, et al., Chem. Mater. **28**, 1128 (2016). https://doi.org/10.1021/acs.chemmater.5b04538